Angewandte Chemie

GDCh

Eine Zeitschrift der Gesellschaft Deutscher Chemiker

www.angewandte.de

Akzeptierter Artikel

Titel: Constructive Nano-Impacts — One by One Synthesis of Individual Nanoparticles

Autoren: Mathies V Evers, Miguel Bernal, Beatriz Roldan Cuenya, and Kristina Tschulik

Zitierweise: *Angew. Chem. Int. Ed.* 10.1002/anie.201813993
Angew. Chem. 10.1002/ange.201813993

Link zur VoR: http://dx.doi.org/10.1002/anie.201813993
http://dx.doi.org/10.1002/ange.201813993

WILEY-VCH

10.1002/ange.201813993

WILEY-VCH

COMMUNICATION

Electrochemical One-by-One Synthesis of Gold Nanoparticles and their Performance in ORR Catalysis

Mathies V. Evers,[a] Dr. Miguel Bernal,[a] Prof. Dr. Beatriz Roldan Cuenya,[b] Prof. Dr. Kristina Tschulik*[a]

Abstract: The impact of individual $HAuCl_4$ nanoreactors is measured electrochemically, which enables *operando* insights and precise control over the modification of electrodes with functional nanoparticles of well-defined size. Uniformly sized micelles are loaded with a dissolved metal salt. Then these solution-phase precursor entities are reduced electrochemically — one by one — to form nanoparticles (NPs). The charge transferred during the reduction of each micelle is measured individually and allows *operando* sizing of each of the formed nanoparticles. Thus, particles of known number and sizes can be decorated homogenously even on non-planar electrodes. This is demonstrated for decoration of cylindrical carbon fibre electrodes with 25 ± 7 nm sized Au particles from $HAuCl_4$-filled micelles. These Au NP-decorated electrodes show great catalyst performance for ORR (oxygen reduction reaction) already at low catalyst loadings. Hence, collisions of individual precursor-filled nano-containers are presented as a new route to nanoparticle modified electrodes with high catalyst utilization, homogeneous particle sizes and surface distribution.

Nanoparticles (NPs) are a major interdisciplinary research field as their synthesis and characterisation continues to pose challenges.[1–3] Since the size is crucial to their properties, the production of monomodal NP batches with narrow size-dispersion is highly desired to maximise catalytic activity and selectivity.[4,5] Simultaneously, costs related to usage of precious metals are reduced. Micelles as templates enable size-selective syntheses. There, a well-defined amount of precursor is confined in a container of specific size. Very uniformly sized micelles can be produced, utilizing diblock copolymers[6,7] and filled with metal salt solutions as precursors. These micellar nano-reactors move about freely in solution and will sporadically collide with an electrode immersed into this solution by virtue of Brownian motion. Here we show that during these individual collisions, the precursor contained inside the micelle[8] can be electrochemically reduced and deposited as a NP at the electrode. The electrochemical charge transferred during each of these impact events allows us to size the formed NPs one by one. The number of events recorded determines the number of NPs formed. Thanks to the random walk driven collisions, a homogeneous coverage of a substrate is achieved during such nano-impacts, even for complex substrate shapes. This is highly desirable to achieve maximum NP utilization in electrocatalysis and sensing.[9]

In literature, the individual impact electroanalysis[10,11] is divided into non-Faradaic capacitive or blocking experiments, and Faradaic catalytic or destructive experiments. These describe the charging, electro-active area decrease, catalysis, and consumption of NPs, respectively.[12–15] In opposition to the categorised procedures, we present the controlled *synthesis* of NPs that occurs in individual events. This tool enables real-time solution-phase analysis of the deposition event at the solid–liquid interface of the electrode.

Conventionally, micellar-confined precursors are reduced chemically using $NaBH_4$, N_2H_4, H_2S, other reductants, or physically by thermal decomposition.[16,17] Major drawbacks of the chemical reduction are the contamination of the resulting NP batch and the difficulty of monitoring the reduction process.[18] Moreover, it is difficult to control and determine the number and individual size of NPs formed upon chemical reduction of micelles *in situ*. In nano-patterning, complex substrate morphology and the limits of galvanic exchange pose limiting factors.[19]

These drawbacks are obliterated in the electrochemical approach used in this work. Precise control of the reduction strength and reaction rate is gained by the applied electrode potential. Instead of a chemical reducing agent, the electrode serves as the electron source with a controlled Fermi level. The reaction is driven for a desired duration, wherein both, number of impacting micelles and transferred charge are monitored. This enables real-time NP size and coverage control. Also, microemulsion droplets, where a second liquid phase is introduced, may be used for this approach,[20–24] However, micelles may be advantageous, as a lower polydispersity index and a longer shelf life can be achieved in comparison to ultrasonication-derived microemulsions.[25] As shown below, the micellar polymer does not measurably influence the catalytic activity in the presented case.

The herein described nanoreactor impact method is aimed as a general method that exceeds the number of metals suitable for galvanic exchange and does not incorporate additional metals which can influence the envisaged application. Further, decoration of any electrically conducting substrate is readily achievable, including non-planar electrodes with high aspect ratios that are not suitable for spin coating, for instance.

We employ the new method of impact electrochemistry to monitor the individual size and number of the deposited NPs in real-time. Using the oxygen reduction reaction (ORR), it is then shown that the modified carbon fibres prepared this way show excellent catalyst performance already at a low gold coverage of ~11 %.

Firstly, micelles of well-defined volume were prepared, filled with a gold precursor and their successful loading and size distribution was determined *ex situ*. See SI section 1 for experimental details.

[a] M. V. Evers, Prof. Dr. K. Tschulik*
Ruhr University Bochum, Faculty of Chemistry and Biochemistry, Chair of Analytical Chemistry II, Bochum, D-44801, Germany
E-mail: Kristina.Tschulik@rub.de
[b] M. Bernal, Prof. Dr. B. Roldan Cuenya
Department of Interface Science
Fritz Haber Institute of the Max Planck Society Berlin, D-14195, Germany

Supporting information for this article is given via a link at the end of the document.

10.1002/ange.201813993

WILEY-VCH

COMMUNICATION

In brief, reverse micelles of the diblock co-polymer P2VP-PS (poly-2-vinylpyridine polystyrene) with adjustable and narrow monomodal size distribution were prepared in toluene, as described by Behafarid *et al.*,[7] and loaded with a precursor by addition of chloroauric acid ($HAuCl_4$). Chloroauric acid is insoluble in toluene and gathers within the micelles, which thus serve as precursor nanoreactor cages. SEM (scanning electron microscopy) and AFM (atomic force microscopy) analysis of $HAuCl_4$@P2VP-PS revealed a nanocage size of 59 ± 10 nm (see Supporting Information **Fig. S1**), which is an order of magnitude smaller and much more well-defined than microemulsion droplets. In order to measure their gold content, micelles were dip-coated on a silicon wafer and treated in oxygen plasma to remove all polymer and form Au NPs.[26] The gold content remained as 21 ± 4 nm individual ligand-free NPs as shown in the AFM image in **Fig. 1**.

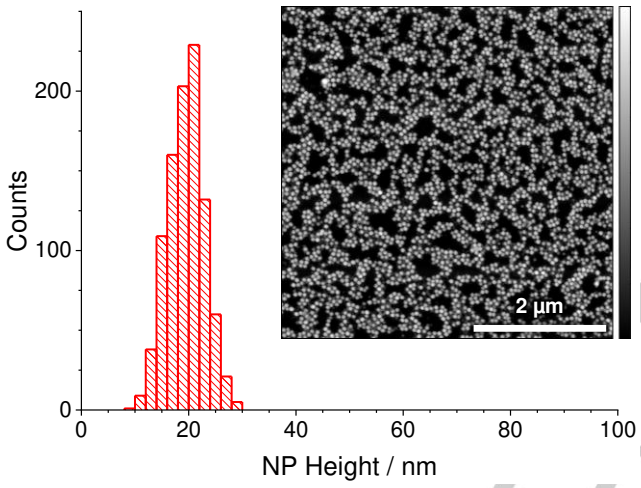

Figure 1. NP height histogram and respective AFM image of O_2-plasma cleaned Au NPs from $HAuCl_4$@P2VP-PS micelles on SiO_2/Si(111) as inset.

Secondly, electrochemical ensemble measurements were used to identify a suitable potential to reduce the precursor ($HAuCl_4$) in the micelles to gold. The inverse micelles were redispersed from toluene into the ionic liquid 1-ethyl-3-methyl-imidazolium bis(trifluoromethylsulfonyl)imide [C_2C_1im][NTf_2], as described in SI Section 1.3. After the removal of toluene, a three-electrode system was introduced to record the linear sweep voltammograms (LSVs) shown in **Fig. 2** on Pt and C microelectrodes. The potential was driven from 0 V vs. a Pt quasi-reference electrode to negative potentials with 0.1 V/s scan rate. On Pt (**Fig. 2A**), the micellar $HAuCl_4$@P2VP-PS is reduced to Au(0) (peak **I**, red) in a single-wave reduction, whereas non-confined $HAuCl_4$ exhibits a double-wave electroreduction (**I** and **II**, black). The reduction of $HAuCl_4$ in micelles (**I**, red) occurs about 300 mV less negatively than without micelles (peak **II** in black). On a carbon electrode (**Fig. 2B**) this difference shrinks to ca. 150 mV. The micelles lead to full electroreduction at an earlier potential which is next used for the individual electrodeposition of nanoparticles in the following paragraph.

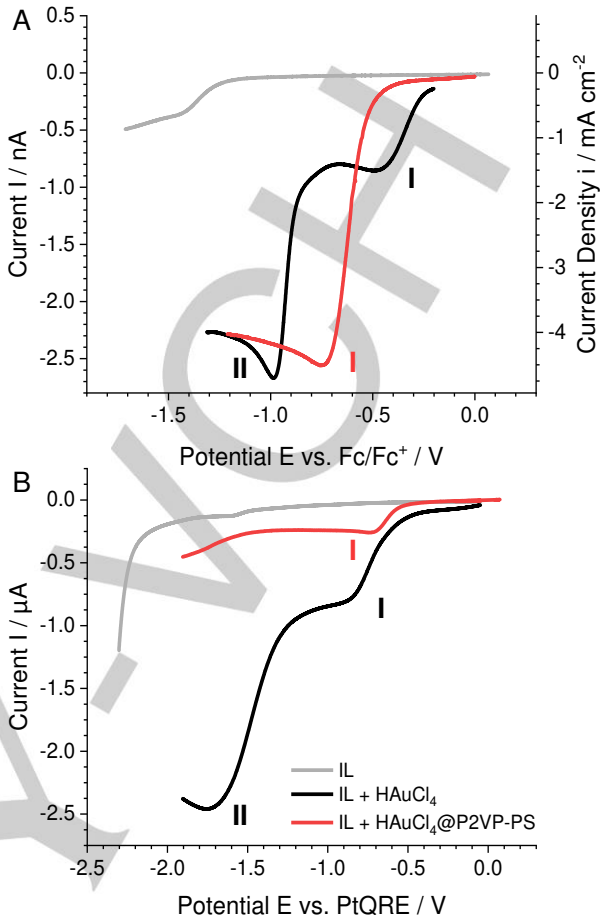

Figure 2. Linear sweep voltammograms of HAuCl4@P2VP-PS micelles in [C_2C_1im][NTf_2]. Scan rate 0.1 V/s. A) LSV at a Pt microdisk (Ø 8 µm), potential referenced against internal redox couple ferrocene/ferrocenium. B) LSV at cylindrical C microfibre (Ø 7.1 µm).

Next, we use nano-impact experiments to synthesise Au NPs from $HAuCl_4$@P2VP-PS micelles, while simultaneously measuring their individual size; a novel synthesis approach we call "constructive nano impacts". There, the micelles were allowed to diffuse in Brownian motion to the electrode. Upon their individual stochastic impact at a negatively polarised Pt microdisk electrode (E = -1.09 V vs. Fc/Fc$^+$, 3-electrode setup), the precursor contained in the micelle was electrochemically reduced. Accordingly, each measured transient current response (spike) marks the electrodeposition of an individual Au NP on the electrode. This reduction spike in the current-time trace is integrated $\int I\,\mathrm{d}t$ to measure the charge Q. In accordance with the reaction equation (1)[27] and Faraday's laws of electrolysis, the charge Q is directly related to the amount of Au(0) deposited. Since the NPs were mostly spherical in shape (see **Figs. 1&3**), the charge directly translated into the diameter d *via* the sphere volume V (2).[28]

$$HAuCl_4 + 3\,e^- \rightarrow Au^0 + H^+ + 4\,Cl^- \qquad (1)$$

$$d = 2 \cdot \sqrt[3]{3V/4\pi} = 2 \cdot \sqrt[3]{(3QM)/(4\pi\rho zF)} \qquad (2)$$

10.1002/ange.201813993

WILEY-VCH

COMMUNICATION

where ρ denotes the density of Au, z the number of transferred electrons, and F the Faraday constant.

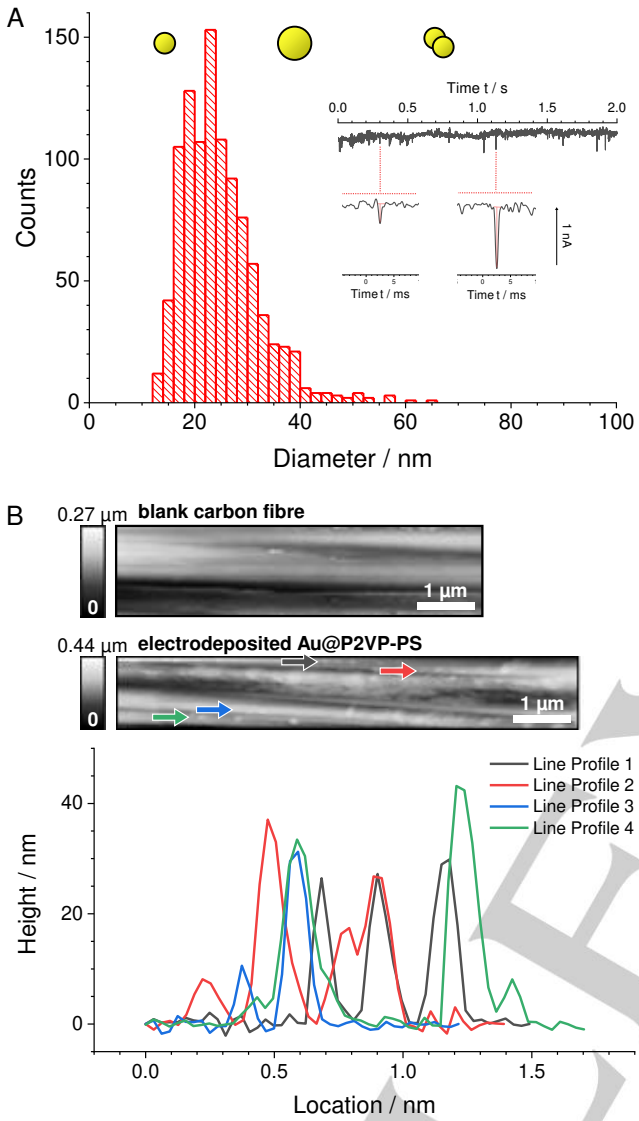

Figure 3. A) Size histogram of NPs electrodeposited by nano impacts on a cylindrical carbon micro fibre; data of 1014 impacts. Inset shows the current transient during an impact measurement and enlarged views of two impact features, additional examples are provided in Figure S4 in the SI. B) AFM image of a cylindrical C fibre before and after impact decoration. C) Baseline-corrected line profiles of the height channel show the size of NPs deposited on the C fibre.

From a total of 1014 *individual* micelle impacts, a size histogram of the formed NPs was plotted. It yields an average diameter of 25 ± 7 nm (**Fig. 3A**). This is in excellent agreement with the Au NP size obtained *ex situ* from plasma-treated micelles (21 ± 4 nm, **Fig. 1**), thus confirming the quantitative conversion of the precursor material in each micelle during nano-impacts. Only few agglomerates are seen at larger diameters. AFM analysis of a cylindrical carbon micro fibre decorated by nano impacts validate the measured size (**Fig. 3B**), which is further confirmed by deposition on a flat substrate (highly oriented pyrolytic graphite, Fig. S3 in the SI).

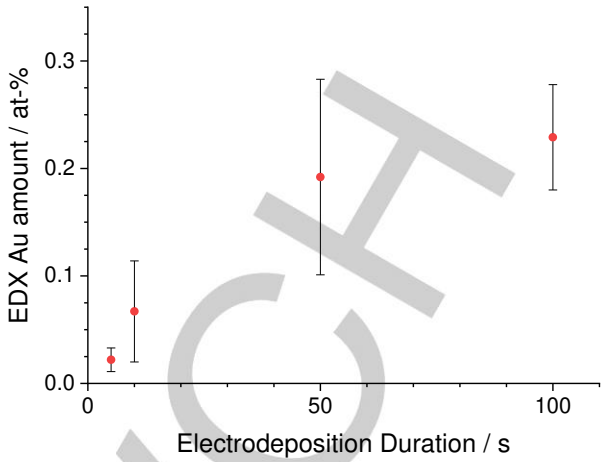

Figure 4. Amount of Au deposition over time after electroreduction of $HAuCl_4$@P2VP-PS micelles on C microfibres; values measured by EDX relative to the detected carbon content (see Section 3.1 in SI).

Constructive impacts were run for a series of deposition times to determine the coverage of a C fibre electrode in dependence of the modification time (**Fig. 4**). We found that the homogeneously deposited amount of Au from $HAuCl_4$@P2VP-PS increased and converged towards saturation up to 100 s. At very long durations a greatly increased amount of Au was observed (see **Fig. S2**). Hence, a limiting "monolayer-type" deposition is assumed, followed by multilayer formation in analogy to classical Brunauer-Emmett-Teller (BET) behaviour. Both, SEM and AFM analysis of the modified electrodes revealed deposited Au NPs of spherical shape. Thus, we demonstrated that $HAuCl_4$@P2VP-PS electrodeposition leads to reproducibly sized particles, which is the opposite for Au NPs from non-confined $HAuCl_4$. Furthermore, the particles adhered strongly to the electrode, allowing us to use the particle-decorated electrodes in catalysis — namely the ORR.

Bulk Au catalyses ORR greatly with respect to blank C fibre electrodes,[29] which is seen from the earlier onset potential at which the reaction starts to show measurable current. Since kinetics of ORR electrocatalysis on Au NPs were studied in detail previously, [29] Au NPs modified carbon micro fibre electrodes are thus utilized in ORR catalysis as a model system herein. First, Au NPs were deposited on a C fibre by micellar nano-impacts and, residual ionic liquid was removed. Next, the decorated fibres were transferred to 0.1 M H_2SO_4 for ORR studies. Using linear sweep voltammetry, the ORR onset potential was determined for Au NPs in comparison to a bare C fibre and a polycrystalline Au electrode, respectively. The measured current was normalized by the surface area, corrected for the hydrogen evolution reaction (HER) in deaerated measurements, and plotted in **Fig. 5**. For the decorated C electrodes, the surface area of the Au NPs which covered 11 % was added to that of the C fibre, to account for the increase of electroactive surface. The onset potential was used as a measure of catalyst performance, and defined as the potential at which the current density reaches -0.05 mA cm^{-2} (**Fig. 5A**). At the respective potential for each material (compare **Fig. 5A** and **Fig. S3.3**), the current is caused mainly by the ORR instead of proton reduction, as verified by blank measurements in deoxygenated solutions. Still, correction of LSVs in O_2-satured solution by those under deaerated conditions in **Fig. 5A** highlights the ORR current, and shows that the onset potential was defined

herein at currents that are kinetically limited and not diffusion-controlled. The unmodified C fibre is denoted as “0 %” catalyst performance and a bulk Au electrode as “100 %”. The performance of the Au NP modified electrode amounted to 62 % of the bulk Au electrode, albeit covering only 11 % of the C surface (**Fig. 5B**). The exceptionally high performance of few, homogeneously distributed NPs is thus clearly demonstrated. Note that this does not prove NPs to be more active than bulk Au, but may (partially) be caused by the efficient hemispherical mass transport of reactants to the individual catalyst NPs. In fact, calculation of the kinetic parameters of our micelle-born Au NPs shows identical catalytic activity for ORR as the capping-agent-free Au NPs reported by Wang *et al.*[29] This confirms that the micellar polymer does not hamper the catalytic activity of the synthesized NPs, as predicted by Behafarid *et al.*[7]

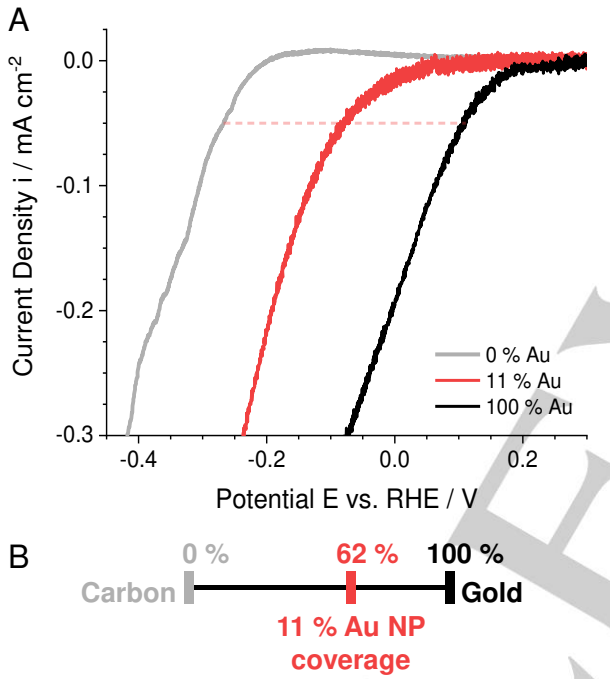

Figure 5. Background-corrected linear sweep voltammograms A) of the ORR at a C fibre electrode (grey), Au electrode (black), and Au NPs supported on a C fibre (red). Scan rate: 0.1 V/s. The horizontal red line indicates the “onset potential” at which the current density equals -0.05 mA cm^{-2}. The scale B) demonstrates the performance as based on the onset potential.

In the present work we demonstrate that micelles can be used as precursor nanoreactor cages to electrosynthesise NPs of narrow size distribution. To homogenously coat Au NPs onto substrate electrodes, we developed and employed the concept of “constructive nano impacts”, which describes the electro-reduction of individual precursor-filled nanoreactors during their impact at the substrate meant to be decorated. This new electrosynthesis tool allows us to deposit NPs one by one and monitor their individual size and the number of NPs formed in situ, based on their individual current response. This approach facilitates the highly efficient utilization of precious metal catalysts, as evidenced for micelle-derived Au NPs in ORR catalysis. At the same time, these modified electrodes are ideal model electrodes for numerical simulations to extract quantitative physicochemical insights on reaction kinetics and mass transport at non-planar electrodes.

As the micelle can be used to store a variety of different precursor substances and mixtures thereof, this novel concept of constructive nano impacts also provides a route to produce a variety of NP-modified electrodes. The monomodal size distribution of the micelles and the homogeneous and precisely adjustable NP surface coverage enable the production of high performance, low cost electrodes for electrocatalytic and electrochemical sensing applications. We anticipate that this will aid improving fuel cells, water purifiers and toxin detectors, amongst other devices.

Acknowledgements

This work was financially supported by the NRW Rückkehrerprogramm and by the Deutsche Forschungsgemeinschaft (DFG) under Germany’s Excellence Strategy EXC-2033 Project-# 390677874 and the Research Training Group ´Confinement-controlled Chemistry´ GRK2376 / 331085229. M.B. acknowledges funding from IMPRS-SURMAT, BMBF under Grant #03F0523C-‘CO2EKAT’ and the ERC under Grant ERC-OPERANDOCAT (ERC-725915).

Keywords: nanoparticle collision experiments • micelles • gold nanoparticles • ionic liquids • oxygen reduction reaction

[1] S. P. Shields, V. N. Richards, W. E. Buhro, *Chem. Mater.* **2010**, *22*, 3212–3225.
[2] E. N. Saw, V. Grasmik, C. Rurainsky, M. Epple, K. Tschulik, *Faraday Discuss.* **2016**, *193*, 327–338.
[3] V. Grasmik, C. Rurainsky, K. Loza, M. V. Evers, O. Prymak, M. Heggen, K. Tschulik, M. Epple, *Chem. Eur. J.* **2018**, *24*, 9051–9060.
[4] R. Reske, H. Mistry, F. Behafarid, B. Roldan Cuenya, P. Strasser, *J. Am. Chem. Soc.* **2014**, *136*, 6978–6986.
[5] H. S. Jeon, I. Sinev, F. Scholten, N. J. Divins, I. Zegkinoglou, L. Pielsticker, B. R. Cuenya, *J. Am. Chem. Soc.* **2018**, *140*, 9383–9386.
[6] A. H. Gröschel, A. Walther, *Angewandte Chemie International Edition* **2017**, *56*, 10992–10994.
[7] F. Behafarid, J. Matos, S. Hong, L. Zhang, T. S. Rahman, B. Roldan Cuenya, *ACS Nano* **2014**, *8*, 6671–6681.
[8] E. Laborda, A. Molina, V. F. Espín, F. Martínez-Ortiz, J. García de la Torre, R. G. Compton, *Angew. Chem. Int. Ed.* **2017**, *56*, 782–785.
[9] X. Li, J. Iocozzia, Y. Chen, S. Zhao, X. Cui, W. Wang, H. Yu, S. Lin, Z. Lin, *Angew. Chem. Int. Ed.* **2018**, *57*, 2046–2070.
[10] K. J. Stevenson, K. Tschulik, *Curr. Opin. Electrochem.* **2017**, *6*, 38–45.
[11] S. V. Sokolov, S. Eloul, E. Kätelhön, C. Batchelor-McAuley, R. G. Compton, *Physical Chemistry Chemical Physics* **2017**, *19*, 28–43.
[12] Z. Deng, R. Elattar, F. Maroun, C. Renault, *Anal. Chem.* **2018**, *90*, 12923–12929.
[13] B. M. Quinn, P. G. van’t Hof, S. G. Lemay, *J. Am. Chem. Soc.* **2004**, *126*, 8360–8361.
[14] X. Xiao, A. J. Bard, *J. Am. Chem. Soc.* **2007**, *129*, 9610–9612.
[15] Y.-G. Zhou, N. V. Rees, R. G. Compton, *Angewandte Chemie International Edition* **2011**, *50*, 4219–4221.
[16] H. Zhao, E. P. Douglas, B. S. Harrison, K. S. Schanze, *Langmuir* **2001**, *17*, 8428–8433.

[17] A. Guiet, T. Reier, N. Heidary, D. Felkel, B. Johnson, U. Vainio, H. Schlaad, Y. Aksu, M. Driess, P. Strasser, et al., *Chem. Mater.* **2013**, *25*, 4645–4652.
[18] M. Wuithschick, B. Paul, R. Bienert, A. Sarfraz, U. Vainio, M. Sztucki, R. Kraehnert, P. Strasser, K. Rademann, F. Emmerling, et al., *Chem. Mater.* **2013**, *25*, 4679–4689.
[19] J. Zhang, Y. Gao, R. A. Alvarez- Puebla, J. M. Buriak, H. Fenniri, *Advanced Materials* **2006**, *18*, 3233–3237.
[20] Y. E. Jeun, B. Baek, M. W. Lee, H. S. Ahn, *Chem. Commun.* **2018**, *54*, 10052–10055.
[21] J. E. Dick, C. Renault, B.-K. Kim, A. J. Bard, *Angew. Chem. Int. Ed.* **2014**, *53*, 11859–11862.
[22] M. W. Glasscott, A. D. Pendergast, J. E. Dick, *ACS Appl. Nano Mater.* **2018**, *1*, 5702–5711.
[23] J. Kim, J. E. Dick, A. J. Bard, *Acc. Chem. Res.* **2016**, *49*, 2587–2595.
[24] B.-K. Kim, A. Boika, J. Kim, J. E. Dick, A. J. Bard, *J. Am. Chem. Soc.* **2014**, *136*, 4849–4852.
[25] H. Deng, J. E. Dick, S. Kummer, U. Kragl, S. H. Strauss, A. J. Bard, *Anal. Chem.* **2016**, *88*, 7754–7761.
[26] H. Tsai, E. Hu, K. Perng, M. Chen, J.-C. Wu, Y.-S. Chang, *Surface Science* **2003**, *537*, L447–L450.
[27] Y.-G. Zhou, N. V. Rees, J. Pillay, R. Tshikhudo, S. Vilakazi, R. G. Compton, *Chem. Commun.* **2011**, *48*, 224–226.
[28] K. Tschulik, B. Haddou, D. Omanović, N. V. Rees, R. G. Compton, *Nano Res.* **2013**, *6*, 836–841.
[29] Y. Wang, E. Laborda, K. Tschulik, C. Damm, A. Molina, R. G. Compton, *Nanoscale* **2014**, *6*, 11024–11030.